Available online at www.sciencedirect.com

ScienceDirect

Ceramics International 40 (2014) 3527–3531

CERAMICS INTERNATIONAL

www.elsevier.com/locate/ceramint

Sol–gel synthesis of Co-doped $LiMn_2O_4$ with improved high-rate properties for high-temperature lithium batteries

Zhenjie Wang[a,b], Junlin Du[a,b], Zhilin Li[a], Zhu Wu[a,*]

[a]*Research Center for New Energy Technology, Shanghai Institute of Microsystem and Information Technology, Chinese Academy of Sciences, Shanghai 201800, China*

[b]*University of Chinese Academy of Sciences, Beijing 100039, China*

Received 2 July 2013; received in revised form 1 September 2013; accepted 17 September 2013
Available online 25 September 2013

Abstract

Co-doped samples are synthesized by a sol–gel method and investigated in detail to improve the high-rate discharge performance of the spinel $LiMn_2O_4$ cathode in high-temperature lithium batteries. The results of X-ray diffraction and scanning electron microscopy confirm that the cobalt additive incorporates into the $LiMn_2O_4$ lattice and that the lattice parameters decrease gradually with increasing Co substitute content. The galvanostatic discharge results indicate that the Co-doped $LiMn_2O_4$ satisfies both high-capacity and high-rate discharge requirements at 200–300 °C when proper substitute contents are chosen. At a high current density of 30 mA cm^{-2}, enhanced high-rate capacities of 219.71 mAh g^{-1} at 200 °C and 307.38 mAh g^{-1} at 300 °C are obtained in $LiMn_{1.7}Co_{0.3}O_4$ and $LiMn_{1.5}Co_{0.5}O_4$, respectively, which have promising applications in high-temperature lithium batteries. These improvements are partly attributed to the enhanced electrical conductivity, as observed through electrochemical impedance spectroscopy.

Keywords: C. Rate performance; D. Cobalt additive; D. Lithium manganate cathode; E. High-temperature lithium battery

1. Introduction

Since the birth of thermal batteries during WW II [1], they have been used as primary power sources for numerous military applications, such as guided missiles and proximity fuzes in ordnance devices. Thermal batteries usually work between 350 and 550 °C; they use an ionically conducting molten salt in the separator between the anode and the cathode [2]. In recent years, great efforts have been exerted to expand the application range of this technology to relatively low-temperature applications such as boreholes. For geothermal and oil/gas exploration, power supplies for measurement while drilling (MWD) equipment in boreholes encounter operating temperatures up to approximately 300 °C [3,4]. Eutectic molten electrolytes, especially nitrates with low melting points, are screened to satisfy the application requirements; the heat of boreholes can automatically melt these electrolytes [3,5,6].

Exothermic reactions occur between nitrate electrolytes and traditional sulfur-based cathode materials in thermal batteries [7]. Thus, oxide-based cathode materials, such as Ag_2CrO_4 and MnO_2, are selected [5,8]. To the best of our knowledge, research on oxide-based cathode materials in high-temperature lithium batteries for borehole applications is insufficient. Given the low melting point (124.5 °C) of the $LiNO_3$–KNO_3 eutectic, previous studies have screened compatible anode and cathode couples to obtain high-capacity and high-rate performances. Miles et al. [9] reported the discharge behavior of cells using Ca anode with $LiNO_3$–KNO_3 eutectic but at relatively low current densities (< 10 mA cm^{-2}). Li (Al)/$LiNO_3$–KNO_3/Ag_2CrO_4 (or V_2O_5) cells were investigated at a current density range of 10–100 mA cm^{-2} but at a temperature range of only 160–215 °C [10]. Considering that the mature Li/$SOCl_2$ technology is limited to temperatures below 200 °C, cells are designed to operate within 200–300 °C, which is included in most envisioned borehole environments. Our previous study [11] dealt with the electrochemical properties of $LiMn_2O_4$ and its Ni-doped derivatives. We found that the voltage plateau and capacities can be effectively improved by partly substituting Ni

*Corresponding author. Tel.: +86 21 69976918; fax: +86 21 32200534.
E-mail address: wuzhu@mail.sim.ac.cn (Z. Wu).

0272-8842/$ - see front matter © 2013 Elsevier Ltd and Techna Group S.r.l. All rights reserved.
http://dx.doi.org/10.1016/j.ceramint.2013.09.076

for Mn. However, the rate discharge performance is as poor as that of the Ni-free spinel. In this research, the rate performance of Co-doped $LiMn_2O_4$ is evaluated, and the performance improvements are preliminarily elucidated.

2. Experimental

2.1. Material preparation and characterization

A series of spinel-type oxide $LiMn_{2-x}Co_xO_4$ (x=0.1, 0.3, 0.5) was synthesized by a sol–gel method. Solutions of acetates of stoichiometric constituent ions and citric acid were mixed. The resulting solution was adjusted to neutral by adding a certain amount of aqueous ammonia. The mixture was magnetically stirred at 80 °C until a clear viscous gel was obtained and then completely dried in a vacuum oven at 90 °C. The precursor was ground and calcined at 400 °C for 8 h and at 700 °C for 20 h continuously. X-ray diffraction (XRD) was performed on a Rigaku D/MAX-2200/PC diffractometer with Cu Kα radiation to determine the phase compositions and lattice parameters. Simultaneous thermogravimetric analysis and differential thermal analysis were performed on a NETZSCH STA 449F3 thermal analyzer to study the chemical compatibility between the cathodes and the $LiNO_3$–KNO_3 eutectic. The morphology of the as-prepared samples was analyzed under a Hitachi S4700 scanning electron microscope.

2.2. Single-cell assembly and tests

The catholyte sample for single-cell assembly and EIS tests consisted of 70 wt% active cathode material, 10 wt% graphite powder (C, CP, 99.85 wt%, Sinopharm) and 20 wt% nitrate eutectic consisting of 33.2 wt% lithium nitrate ($LiNO_3$, AR, 99.0 wt%, Sinopharm) and 66.8 wt% potassium nitrate (KNO_3, GR, 99.0 wt%, Sinopharm). The electrolyte consisted of 65 wt % $LiNO_3$–KNO_3 eutectic and 35 wt% MgO by melt blending at 300 °C for 16 h. Single cells were assembled by stacking a 0.20 g LiMgB pellet (58 wt% Li, 4 wt% Mg, and 38 wt% B) and a bilayer pellet consisting of 0.30 g each of depolarizer–electrolyte and electrolyte binder layers pressed at 222 MPa. Galvanostatic discharge measurements were performed on a LAND potentiostat/galvanostat at 200 and 300 °C at current densities of 10 and 30 mA cm^{-2}, respectively. The cell discharge was terminated when the voltage dropped below 1.00 V. The electrical conductivities of the catholytes were measured at 200–300 °C by electrochemical impedance spectroscopy (EIS) on a CHI660D (Chenhua) electrochemical workstation in the frequency range of 100 kHz to 0.01 Hz.

3. Results and discussion

3.1. Material characterization

Fig. 1 shows the XRD patterns of the $LiMn_{2-x}Co_xO_4$ samples. All Co-doped samples are in agreement with the standard pattern of spinel $LiMn_2O_4$ below. Similar to the Ni-doped derivatives [11], they are all identified as a single pure phase of cubic spinel structure in the Fd-3 m space group without any impurity phases. Moreover, the ionic radius of Co^{3+} (0.545 Å) is closer to that of Mn^{3+} (0.645 Å) than that of Li^+ (0.76 Å). Thus, the cobalt additive incorporates into the $LiMn_2O_4$ lattice and partly occupies the octahedral (16d) site of manganese ions rather than the Li^+ site. In addition, the diffraction peaks gradually shift toward the large-angle direction with increasing Co substitute content. This result suggests that the lattice parameters decrease accordingly, which is ascribed to the smaller ionic radius of Co^{3+}. This finding also agrees with the refinement results shown in Table 1. With decreasing Mn^{3+}, the resulting Jahn–Teller effect and disproportionate reaction are effectively suppressed. Consequently, the stability of the lattice structure is improved for the Co-doped $LiMn_2O_4$.

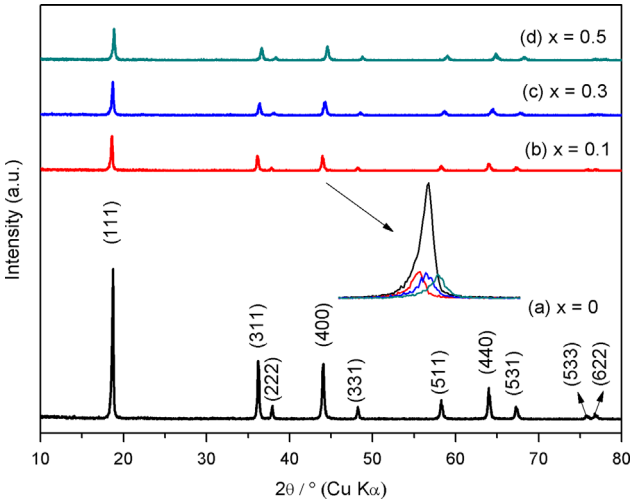

Fig. 1. XRD patterns of $LiMn_{2-x}Co_xO_4$.

Table 1
Lattice parameters of $LiMn_{2-x}Co_xO_4$ spinels.

Sample	Lattice Parameter, a (Å)	Unit Cell Volume (Å^3)
$LiMn_2O_4$	8.22281[11]	555.98[11]
$LiMn_{1.9}Co_{0.1}O_4$	8.21442	554.28
$LiMn_{1.7}Co_{0.3}O_4$	8.16837	545.01
$LiMn_{1.5}Co_{0.5}O_4$	8.12764	536.90

Moreover, obvious broadening of the XRD peaks is observed in the enlarged X-Ray diffraction diagrams, such as the (400) crystal face shown in the inset. On the basic of the broadening [12], the particle sizes of as-prepared samples are calculated using Scherrer equation:

$$D = \frac{K\lambda}{(B\ \cos(\theta))} \quad (1)$$

where D is the average particle size, K is a constant, λ is the wavelength of the X-ray radiation, B is the broadening of the diffraction line measured at half maximum intensity and θ is the Bragg angle. Using this method, the particle sizes obtained by the Jade software are 45.0 nm, 42.3 nm, 31.9 nm and 34.3 nm which basically show a trend of decline with increasing Co content.

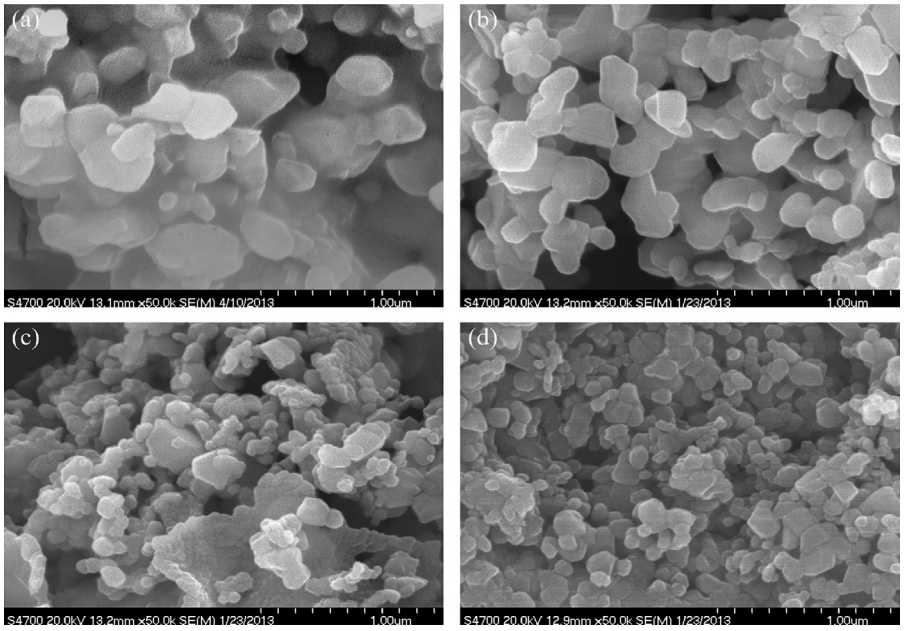

Fig. 2. SEM images of $LiMn_{2-x}Co_xO_4$ ((a) $x=0$, (b) $x=0.1$, (c) $x=0.3$, and (d) $x=0.5$).

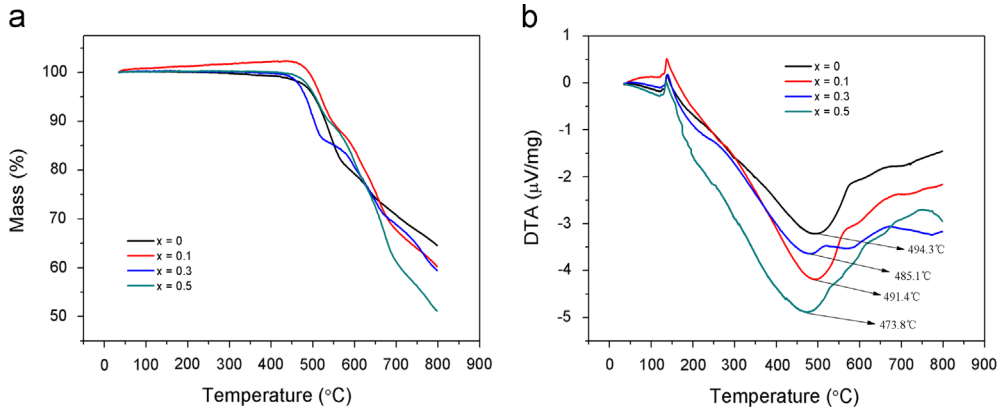

Fig. 3. TG/DTA curves of $LiMn_{2-x}Co_xO_4$/ $LiNO_3$–KNO_3 eutectic mixtures.

The microstructural features of the as-prepared $LiMn_{2-x}Co_xO_4$ spinels are shown in Fig. 2. All samples present homogeneous irregular-shaped particles and no significant difference with Co additive is observed, except for changes in particle size. As expected, the grain size decreases significantly with increasing Co substitute content, which is quite in agreement with particle size calculated from XRD results above. This corresponding relation is similar with the $Bi_{1-x}Ba_xFeO_3$ samples [12].

Fig. 3 shows the thermal analyses of different $LiMn_{2-x}Co_xO_4$/$LiNO_3$–KNO_3 eutectic mixtures from room temperature to 800 °C. Compatibility analysis is performed before discharge to avoid thermal runaway and other security issues in batteries resulting from exothermic reactions. The combinations are all thermally stable at around 450 °C. The only endothermic peak appeared at around 136 °C for each sample. This peak corresponds to the melting process of the $LiNO_3$–KNO_3 eutectic. At elevated temperatures, exothermic reactions occur between the spinel cathodes and nitrates coupled with significant mass loss. The temperatures of the initial exothermic reactions between the samples and nitrates show significant decrease as Co concentration increases, which indicates that the Co doping has some catalysis effect on the reactions, in other words, making them easier. As mentioned above, the particle size decreases with increasing Co concentration, so the specific surface area increases accordingly, which efficiently improves the surface energy for the active cathode materials. As a result, the reactions between the cathodes and nitrates become easier and easier, reflected in the decrease of the initial reaction temperatures. Thus, the cell combinations are not suitable for applications at or above 450 °C, but safety is guaranteed for boreholes envisaged below 300 °C.

3.2. Electrochemical tests

Galvanostatic discharge tests are performed at different current densities in a temperature range of 200–300 °C. The results are shown in Figs. 4 and 5 and in Table 2. Galvanostatic discharge

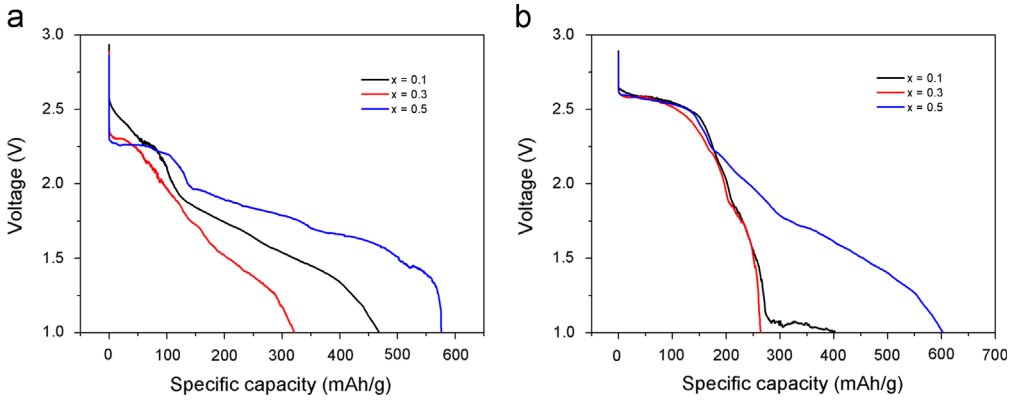

Fig. 4. Galvanostatic discharge curves of $LiMn_{2-x}Co_xO_4$ (x=0.1, 0.3, 0.5) at a current density of 10 mA cm^{-2} at temperatures of (a) 200 °C and (b) 300 °C.

Table 2
Galvanostatic discharge results for the $LiMn_{2-x}Co_xO_4$ cathodes.

Sample	Specific Capacity/mAh g^{-1} (10 mA cm^{-2})		Specific Capacity/mAh g^{-1} (30 mA cm^{-2})		Capacity Retention (30 mA cm^{-2}:10 mA cm^{-2})	
	200 °C	300 °C	200 °C	300 °C	200 °C	300 °C
$LiMn_2O_4$	340.52[11]	237.43[11]	75.33	116.67	0.22	0.49
$LiMn_{1.9}Co_{0.1}O_4$	468.48	402.05	73.76	153.90	0.16	0.38
$LiMn_{1.7}Co_{0.3}O_4$	321.05	264.05	219.71	270.62	0.68	1.02
$LiMn_{1.5}Co_{0.5}O_4$	576.05	602.81	161.38	307.38	0.28	0.51

results at 10 mA cm^{-2} for the Co-free $LiMn_2O_4$ have been reported in our previous work [11]. As shown in Fig. 4, these cells have an open-circuit voltage of almost 3 V, and the Co-doped cathodes present much higher capacities than the Co-free $LiMn_2O_4$ cathode at a current density of 10 mA cm^{-2}. The highest capacities of 576.05 and 602.81 mAh g^{-1} at 200 and 300 °C, respectively, both appear in the $LiMn_{1.5}Co_{0.5}O_4$ cathode. In addition, $LiMn_{1.5}Co_{0.5}O_4$ presents a much higher and wider voltage plateau, which facilitates high-rate discharge. The rapid decline of the voltage plateau for these three cathodes at 300 °C is ascribed to the improved self-discharge at higher temperatures. The specific reaction mechanisms related to the distinct voltage plateau are identified as step-by-step lithium intercalation processes, which have been elucidated in our earlier work [11].

At the improved current density of 30 mA cm^{-2}, severe performance degradation occurs with respect to discharge capacities and voltage plateau. The distinct voltage plateau for all cathodes are less than 2.0 V, which is lower than the higher plateau of around 2.5 V at 10 mA cm^{-2}. The Co-free $LiMn_2O_4$ presents diminished high-rate capacities of 75.33 and 116.67 mA cm^{-2} at 200 and 300 °C, respectively, that is, poor retentions of only 0.22 and 0.49 are obtained compared with those at 10 mA cm^{-2}. However, the highest discharge capacities at 200 and 300 °C are 219.71 mAh g^{-1} for $LiMn_{1.7}Co_{0.3}O_4$ and 307.38 mAh g^{-1} for $LiMn_{1.5}Co_{0.5}O_4$, respectively. Moreover, the $LiMn_{1.7}Co_{0.3}O_4$ cathode exhibits the highest capacity retention at both temperatures. In general, the Co additive leads to high-rate discharge capacities. As stated previously, the lattice parameters decrease with increasing Co content, resulting in larger specific surface area. The large specific surface area facilitates greater contact between the active cathode surface and the electrolyte, and then decreases concentration polarization at high rates [13].

Compressing powder discs for pure $LiMn_{2-x}Co_xO_4$ powders is difficult. Thus, EIS analysis is performed on catholytes consisting of active cathode, nitrate eutectic, and graphite whose electrical conductivities are much higher than those of the pure samples. The differences between them are mainly determined by $LiMn_{2-x}Co_xO_4$. Up to 0.50 g of each catholyte powder is pressed at 222 MPa and tested at 200 and 300 °C to reflect the actual discharge situation in batteries. The electronic conductivity is calculated by the following formula:

$$\sigma = l/(R_b A)\ (\mathrm{S\ cm^{-1}}) \quad (2)$$

where σ is the electronic conductivity of the catholyte, l is the thickness of the disc, R_b is the resistance of the catholyte obtained by EIS, and A is the cross-sectional area of the disc. The relationship curves of electronic conductivity vs. Co content (x) are shown in Fig. 6.

As shown in Fig. 6, the electronic conductivities at 300 °C are much higher than those at 200 °C. Thus, the degraded performance indicates increased self-discharge at higher temperature. Compared with the Co-free catholyte, catholytes consisting of Co additive present higher electronic conductivities. The electronic conductivities show an increasing tendency as the Co substitute content increases, which basically agree with changes in discharge capacities. The highest electronic conductivity at 300 °C appears in $LiMn_{1.5}Co_{0.5}O_4$,

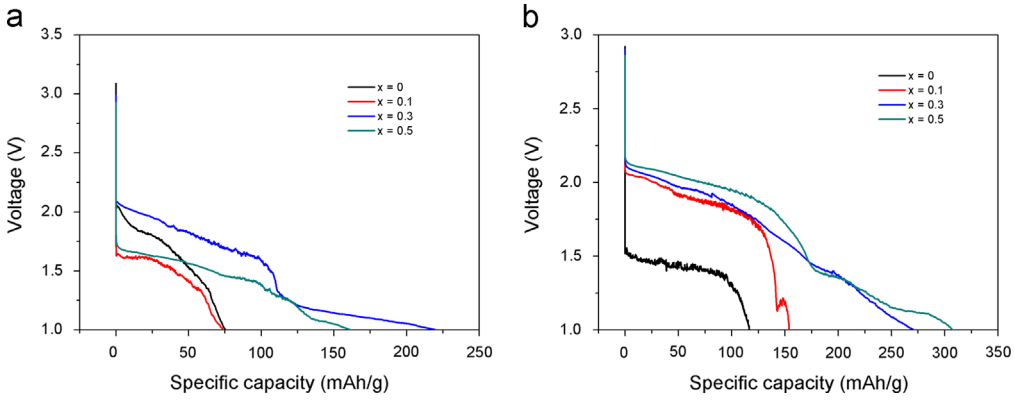

Fig. 5. Galvanostatic discharge curves of $LiMn_{2-x}Co_xO_4$ (x=0, 0.1, 0.3, 0.5) at a current density of 30 mA cm^{-2} at temperatures of (a) 200 °C and (b) 300 °C.

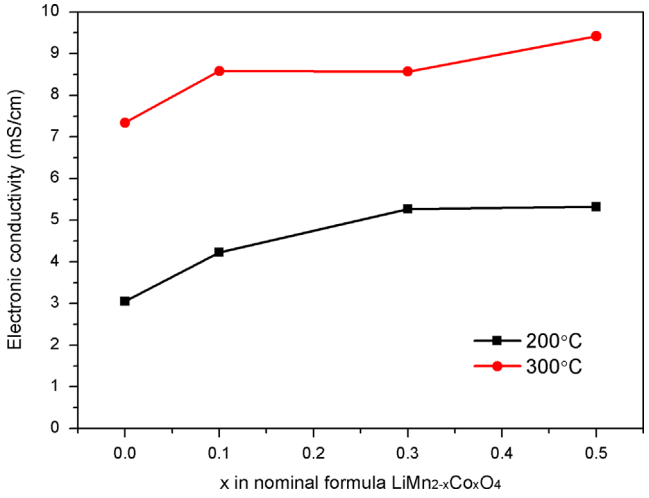

Fig. 6. Electronic conductivities of $LiMn_{2-x}Co_xO_4$ (x=0, 0.1, 0.3, 0.5).

which also possesses the highest capacity and voltage plateaux at a high rate. The $LiMn_{1.7}Co_{0.3}O_4$ cathode with the best high-rate performance at 200 °C also has a relatively high conductivity. Therefore, aside from the self-discharge, the high-rate discharge performance of the spinel $LiMn_{2-x}Co_xO_4$ is strongly influenced by its electronic conductivity.

4. Conclusions

Co-doped $LiMn_{2-x}Co_xO_4$ powders are successfully synthesized via a sol–gel method. The chemical compatibility between these cathodes and the nitrate eutectic are demonstrated below 450 °C. The Co-doped samples have smaller lattice parameters and greater specific surface area than the Co-free $LiMn_2O_4$. The highest rate capacities at 30 mA cm^{-2} are 219.71 mAh g^{-1} at 200 °C and 307.38 mAh g^{-1} at 300 °C, respectively, which are much higher than that of the Co-free $LiMn_2O_4$. The EIS results demonstrate that Co-doping effectively improves electronic conductivity, leading to high-rate performance at certain temperatures.

Acknowledgments

This work was financially supported by the Scientific Research Project of the Science and Technology Commission of Shanghai Municipality (09dz1206800).

References

[1] W.E. Kuper, A brief history of thermal batteries, in: Proceedings of the 36th Power Sources Conference, 1994, pp. 300–309.
[2] R.A. Guidotti, P.J. Masset, Thermally activated ("thermal") battery technology Part I: an overview, Journal of Power Sources 161 (2006) 1443–1449.
[3] R.A. Guidotti, F.W. Reinhardt, J. Odinek, Overview of high-temperature batteries for geothermal and oil/gas borehole power sources, Journal of Power Sources 136 (2004) 257–262.
[4] P.J. Masset, R.A. Guidotti, Thermal activated ("thermal") battery technology-Part IIIa: FeS_2 cathode material, Journal of Power Sources, 177, 595–609.
[5] R.A. Guidotti, F.W. Reinhardt, Performance of Li-alloy Ag_2CrO_4 couples in molten $LiNO_3$–KNO_3 eutectic electrolyte, in: Proceedings of the 36th Intersociety Energy Conversion Engineering Conference, 2002, pp. 31–42.
[6] M.H. Miles, Electrochemistry of molten nitrate electrolytes and applications for high voltage lithium cells, Electrochemical Society Proceedings 21 (2001) 557–563.
[7] R.A. Guidotti, High-temperature batteries for geothermal and oil–gas borehole applications, in: Proceedings of the Energy Conversion Engineering Conference and Exhibit, 2000, pp. 1276–1286.
[8] R.A. Guidotti, F.W. Reinhardt, Evaluation of the Li (Al)–MnO_2 couple in $LiNO_3$-KNO_3 eutectic electrolyte for borehole applications, in: Proceedings of the 41st Power Sources Conference, 2002, pp. 141–144.
[9] M.H. Miles, D.A. Fine, A.N. Fletcher, The calcium anode in molten nitrate electrolytes, Journal of the Electrochemical Society 125 (1978) 1209–1214.
[10] C.O. Giwa, Feasibility study of materials for a medium-temperature reserve cell concept, Materials Science Forum 73 (1991) 699–706.
[11] Z.J. Wang, J.L. Du, W.Y. Duan, Y.Q. Niu, Z. Wu, $LiMn_{2-x}Ni_xO_4$ spinel oxides as high-temperature lithium battery cathode materials for borehole applications, International Journal of Electrochemical Science 8 (2013) 6231–6242.
[12] S. Chauhan, M. Arora, P.C. Sati, S. Chhoker, S.C. Katyal, M. Kumar, Structural, vibrational, optical, magnetic and dielectric properties of $Bi_{1-x}Ba_xFeO_3$ nanoparticles, Ceramics International 39 (2013) 6399–6405.
[13] X.Y. Lai, J.E. Halpert, D. Wang, Recent advances in micro-/nano-structure hollow spheres for energy applications: from simple to complex systems, Energy Environment Science 5 (2012) 5604–5618.